**RAA 2017** Vol. **17** No. **9**, 97 (10pp) doi: 10.1088/1674–4527/17/9/97

*http://www.raa-journal.org* *http://iopscience.iop.org/raa*

***R**esearch in*
***A**stronomy and*
***A**strophysics*

# Frequency drift rate of solar decameter "drift pair" bursts

Aleksander Stanislavsky[1,2], Aleksander Konovalenko[1] and Yaroslav Volvach[1]

[1] Institute of Radio Astronomy, Kharkiv 61002, Ukraine; *alexstan@ri.kharkov.ua*
[2] V.N. Karazin Kharkiv National University, Kharkiv 61002, Ukraine

Receive 2016 December 18; accepted 2017 June 14

**Abstract** This paper deals with the detailed analysis of frequency drift rates of solar "drift pair" (DP) bursts observed from 2015 July 10 to 12 during a type III burst storm. The observations were conducted by the UTR-2 radio telescope at 9–33 MHz with high frequency and time resolution. DPs were recorded drifting from higher to lower frequencies (forward DPs) as well as from lower to higher ones (reverse DPs). Patterns on their dynamic spectrum had various inclines and occupied different bandwidths. The frequency drift rate versus frequency dependence of these bursts has been studied. The fitting model to describe the peak evolution of these bursts in the frequency-time plane is presented. The relationship between DPs and type III solar bursts is discussed.

**Key words:** Sun: corona — Sun: radio radiation — methods: observational — techniques: spectroscopic

## 1 INTRODUCTION

Studies of solar "drift pair" (DP) bursts were launched with the pioneering work of Roberts (1958). He was the first who drew attention to a special form of radiation observed from the solar corona. Each of these bursts consisted of two short components separated in time, the second repeating the first on dynamic spectra of the radio emission. DPs are relatively rare events which occur during some solar storms of type III bursts (de La Noe & Moller Pedersen 1971). They drift from high frequencies to low ones and visa versa. The main outcome from the DP studies of Moller-Pedersen et al. (1978) and de La Noe & Moller Pedersen (1971) is the quantitative measurements of observational characteristics (including the drift rates) and statistics in the frequency ranges 25–75 MHz and 20–80 MHz, respectively. Also McConnell (1982) noticed a great resemblance of DPs to S bursts in terms of properties. Attempts to find an explanation for this manifestation of solar activity have been taken by the scientific community many times, but they left more questions than answers. The latest review of progress in the experimental and theoretical investigations of DPs was presented in Melnik et al. (2005).

One of the key problems, connected with DPs, is how their frequency drift rate varies with frequency. This dependence is very important for understanding the origin of such bursts. At the present time there are two different points of view on this dependence. According to Moller-Pedersen et al. (1978), at 20–80 MHz the DP frequency drift rate as a function of frequency was described by the following formula

$$\dot{f} = |-0.17f + 3.4|\,, \tag{1}$$

where, as usual, the dotted symbol means the first-order derivative in time. However, the experimental results of Melnik et al. (2005) demonstrated another dependence, namely

$$\dot{f} = A(f/f_0)^B + C\,, \tag{2}$$

where $A$, $B$ and $C$ are the fitting parameters, and $f_0 = 25$ MHz. According to the least-squares approximation, the parameters had the following values: $A = -0.5$, $B = 2.7$ and $C = -0.4$ for forward DPs (FDPs); whereas for reverse DPs (RDPs) $A = 2.3$, $B = 6.2$ and $C = 1$. Note that 774 DPs were recorded during the observations. Moreover, the authors have paid special attention to the study of DP drift rates at decameter wavelengths. On such a basis, they assumed that the DP radio emission could originate from the interaction between fast magnetosonic waves and type III Langmuir waves. Unfortunately, further detailed development of the proposed ideas was not accomplished. Recently, we have

carried out new independent observations of solar DPs to bring greater clarity to this problem. This paper presents new results devoted to the experimental study of DPs in low frequencies.

## 2 FACILITIES AND OBSERVATIONS

### 2.1 UTR-2 Radio Telescope

Our solar observations were performed between 2015 July 10–12 by the UTR-2 radio telescope (see details in Braude et al. 1978, Konovalenko et al. 2016) located around 70 km from Kharkiv in Ukraine. The instrument allows us to receive radio emission in the continuous frequency band of 9–33 MHz with high frequency, time and angular resolution. It should be mentioned that similar observations of DPs were implemented by using this antenna in July 2002 (Melnik et al. 2005), but in our case the recording equipment was more advanced (see details below).

The UTR-2 antenna generally consists of 2040 wideband horizontal dipoles distributed over 12 sections. In 2002 three sections of the UTR-2 were used, and the radio data were recorded independently by an analog multichannel receiver (10–30 MHz), tuned to 60 selected frequencies with frequency bandwidth 3 kHz in each frequency channel (with time resolution 50 ms), and by the Digital Spectral Polarimeter (DSP), which carried out fast Fourier analysis in the continuous frequency band 17.6–29.8 MHz with frequency and time resolution of 12 kHz and 100 ms respectively. Most results of Melnik et al. (2005) were recorded by the analog multichannel receiver. The frequency gaps between neighboring frequency channels in the 60-channel spectrometer (i.e. from 110 kHz to 1.4 MHz) depend on the radio interference environment between 10 MHz and 30 MHz. The recorded solar data reported in this work are entirely digital and broadband observations. Also we used four sections of the UTR-2 antenna array covering a total effective area of 50 000 $m^2$. This is sufficient to detect solar bursts at these frequencies due to characteristics of the antenna radiation pattern.

### 2.2 Digital Receiver for Radio Astronomy Applications

Solar data from the UTR-2 antenna array were recorded by a new two-channel digital receiver/spectrometer (Ryabov et al. 2010) in which the working parameters can be tuned to optimize the reception of both sporadic and stationary types of radio signals. This instrument executes a fast Fourier transform of received signals in the full frequency band (9–33 MHz) of the UTR-2 radio telescope. As applied to our observations, the solar radiation was registered with a time resolution of 50 ms and a frequency resolution of 4 kHz. Due to the very high dynamic range of this equipment (about 90 dB), weak signals in the background of strong ones were detected without any distortion. This situation just takes place in the case of DPs that are superposed on the background of stronger type III bursts. The sensitivity of our equipment was about 0.012 sfu (1 sfu = $10^{-22}$ W $m^{-2}$ $Hz^{-1}$) at 25 MHz (Stanislavsky et al. 2009) and was about 0.018 sfu for the same frequency in 2002. For comparison, the flux of DP bursts was from tens to some hundreds of sfu. It should be recalled also that in the UTR-2 frequency range the system noise temperature is produced basically by Galactic background radiation. The noise temperature is about 28 300 K at 25 MHz (Krymkin 1971), and higher at lower frequency.

### 2.3 Solar Events Associated with DPs

The occurrence of DPs and the storm of type III bursts in 2015 July 10–12 (see Fig. 1) were associated with active regions on the solar disk. At that time the most active region was NOAA AR 12381 (N14W25 on 2015 July 10). One day before it was located near the central meridian (see more details in *http://www.solarmonitor.org/*). The sunspot group belonged to the magnetic $\beta$ class, having both positive and negative magnetic polarities with a simple division between them. The solar activity was accompanied by rare solar X-ray flares of C class. Our daily solar observations were conducted in summer and lasted about four hours before and after the meridian transit.

## 3 DATA ANALYSIS

During 2015 July 10–12, we obtained the data of 301 DP bursts from which 209 were forward (FDPs) and 92 were reverse (RDPs). However, the bursts are similar in appearance to dynamic spectra (Fig. 1) but differ in observational parameters like frequency bandwidth, starting and ending frequencies and time duration and frequency drift-rates.

### 3.1 Frequency Bandwidth

One of the interesting DP parameters is the total frequency bandwidth occupied by each such burst. We have analyzed the characteristics of FDPs and RDPs measured on 2015 July 10–12 (see the bottom panels of Fig. 2). The average value of the frequency bandwidth was $2.82 \pm 1.32$ MHz for RDPs, whereas for FDPs

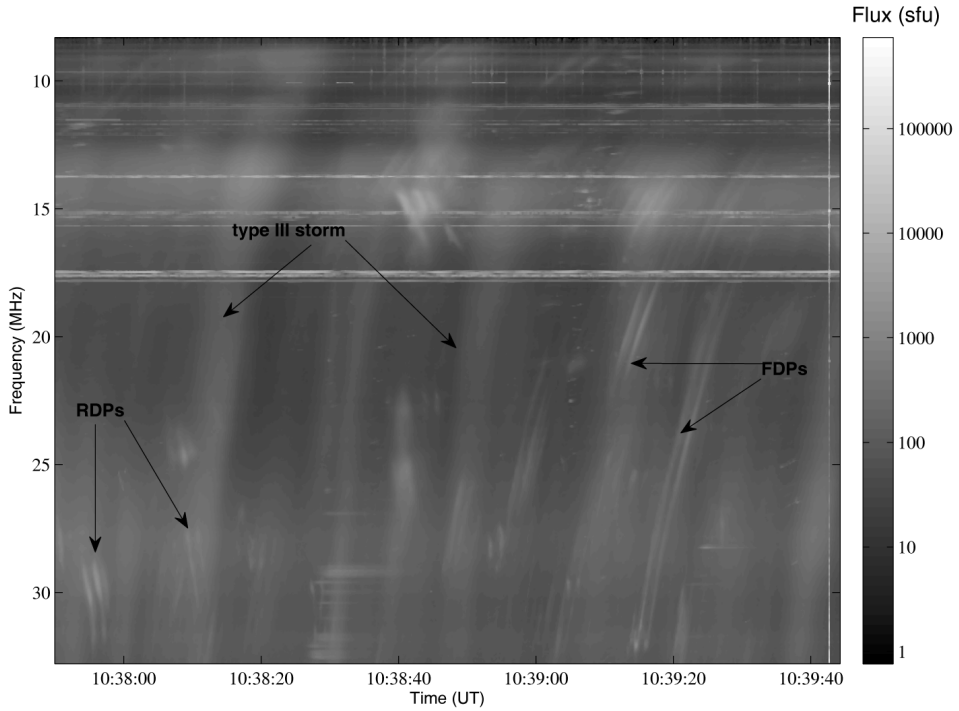


**Fig. 1** Dynamic spectrum of the drift-pair bursts superposed on type III bursts obtained from the UTR-2 observations on 2015 July 11. The data are calibrated (1 sfu = $10^{-22}$ W m$^{-2}$ Hz$^{-1}$).

it was 3.6±2.4 MHz. It is important to note that our observations on those days have clearly showed that high-frequency edges of long DPs were located upward in the frequency band of the UTR-2 radio telescope. Unfortunately, the given observations do not permit us to record radio emission in the whole frequency band, where the DPs originate. This imposes restrictions on our measured results.

As can be easily seen in Figure 2, within the frequency range of observations of our instrument, the number of FDPs decreases at high frequencies, whereas the number of RDPs is reduced towards lower frequencies. These histograms also reveal that the number of RDPs increases in the direction of high frequencies, and FDPs show a similar trend towards low frequencies. This peculiarity can be characterized by the skewness that is a measure of the asymmetry in probability distributions. The parameter of FDPs is equal to 0.237 whereas for RDPs it is −0.966. Unfortunately, the frequency range of the DP observations was not enough to study the distributions of FDPs and RDPs completely. Nevertheless, this explains why, in the observations of de La Noe & Moller Pedersen (1971), about 30% of observed DPs were FDPs and the rest were RDPs. It was not surprising that in Melnik et al. (2005) the quantitative relation between FDPs and RDPs for the UTR-2 observations was vice versa: 109 and 89 on July 13, and 186 and 123 on July 14, respectively. In this context any observation at lower frequencies (than was done previously) would be interesting for the analysis of FDPs. However, capabilities of the ground-based instruments are limited by ionospheric cutoff effects. The spacecraft investigations do not give acceptable resolutions in time and frequency for the study of DPs, and their sensitivity is not sufficiently high because of the simple antennae on board (see Stanislavsky et al. 2009). One may hope that future observations will be available for a lunar radio array landed on the lunar farside surface that can be used for ultra-long wavelength radio astronomy (see, for example, Jester & Falcke 2009). As for higher frequency observations, they would be useful for in-depth study of RDPs. This might help new low-frequency radio telescopes that are in development (Konovalenko et al. 2016 and references therein).

The first once-over of the histograms presented in Figure 2 allows us to see a frequency shift between the distributions of upper and lower frequencies for both FDPs and RDPs. This may indicate a linear regression between the random variables (Feller 2008). The correlation between starting and ending frequencies in each group of DPs is close to one (0.92 for FDPs and 0.96 for RDPs). In this case a linear relationship can be considered as

$$f_{2F} = 1.12\, f_{1F} + 1.33\,, \qquad (3)$$

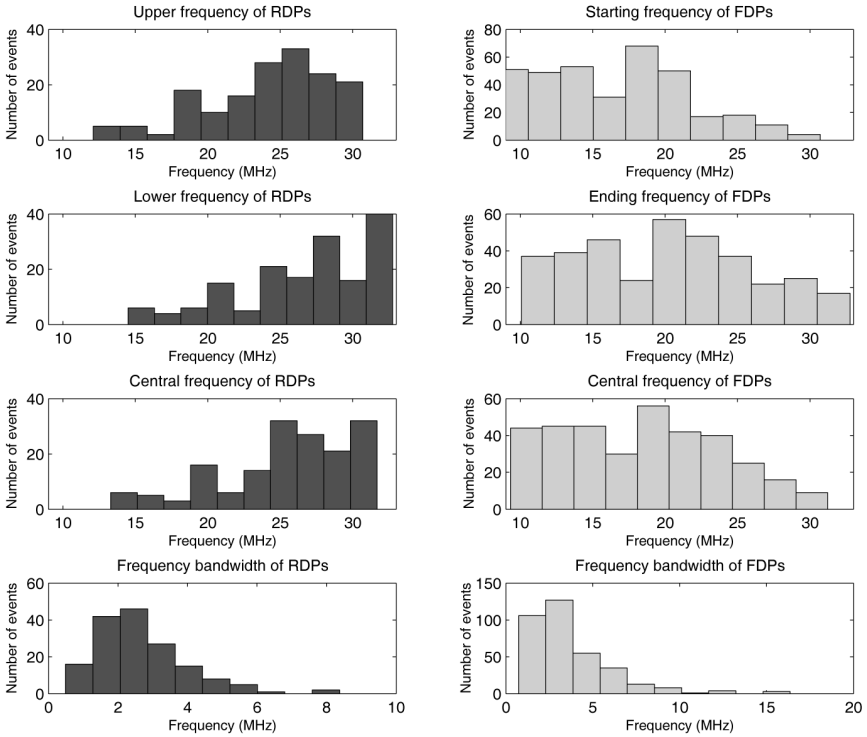


**Fig. 2** Histograms representing statistical properties of FDPs and RDPs obtained from the solar observations on 2015 July 10–12.

$$f_{2R} = 1.05\, f_{1R} + 1.14\,, \tag{4}$$

where $f_1$ is the starting frequency, $f_2$ is the ending one, and the additional subscripts $F$ and $R$ denote each set of solar bursts (FDPs and RDPs, respectively). It should be noticed that the FDP (or similarly RDP) bandwidth also satisfies the linear model $\Delta f_F = 0.12\, f_{1F} + 1.33$ (and $\Delta f_R = 0.05\, f_{1R} + 1.14$ for RDPs). Moreover, we have identified outliers in the data. Probably, their appearance is related to the fact that some DPs were cropped in frequency above and/or below because of the instrumental capability to observe at 9–33 MHz. In this connection it should be mentioned also that using the Culgoora spectropolarimeter, Suzuki & Gary (1979) have identified 366 RDPs from 24.7 MHz to 74 MHz. Their analysis demonstrated the apparent abrupt fall in the number of RDPs at low frequency that were explained by the radio interference from short-wave transmitters below about 30 MHz. The histograms of frequencies, at which each RDP began and ended, have a marked tendency for peaks in the starting frequency histogram to shift with respect to the ending frequency histogram. As the histograms are very similar, this could indicate a linear regression relationship between starting and ending frequencies of the RDPs. The frequency bandwidth of the bursts had a peak at 4 MHz, and the number of RDPs rapidly fell off for 8 MHz. The authors also noticed that the narrow-band RDPs (with frequency bandwidth less 4 MHz) were difficult in identify on spectrograph records, as the experimental data were truncated at low frequencies.

This gives evidence that the random variables $f_{1F}$ and $f_{2F}$ (as well as another pair $f_{1R}$ and $f_{2R}$) have the same probability density function (PDF). Considering the histograms of DP bandwidth and drawing their quantile-quantile plot, we have found that the PDF is an example of a Pearson III type distribution (Singh 1998). The distribution is also called the shifted gamma distribution and is written as

$$g(y) \;=\; \frac{1}{b\Gamma(a)} \left(\frac{y-m}{b}\right)^{a-1} \exp\left[-\frac{y-m}{b}\right] \mathbb{1}_{(m,\infty)}\,, \tag{5}$$

where $a > 0$ is the shape parameter, $b > 0$ the scale parameter and $m$ the location (or shift) parameter. Recall that the change $\frac{Y-m}{b}$ transforms the random variable $Y$ into the random variable following the two-parameter gamma PDF with scale parameter equal to one. As the records of these sequences $(y_1, \ldots, y_n)$ are available, our next objective is to estimate the parameters $(a, b, m)$ of this distribution in both cases of DPs.

The maximum likelihood method and the method of moments are commonly used to calculate $(\hat{a}, \hat{b}, \hat{m})$ of $(a, b, m)$ (Johnson et al. 1970). The method of moments is more preferable because the maximum likelihood method becomes unstable for some values of $a$, especially for truncated data. To determine the parameters $(a, b, m)$ from our experimental data, it suffices to find the mean $\mu = E[Y] = m + ab$, variance $\sigma^2 = E[Y^2] - \mu^2 = ab^2$ and skewness $\gamma = E[(Y - \mu)^3]/\sigma^3 = \frac{2|b|}{b\sqrt{a}}$. These relationships with $\mu$, $\sigma$ and $\gamma$ are replaced by their estimates $\hat{\mu}$, $\hat{\sigma}$ and $\hat{\gamma}$ respectively to obtain estimates of $(a, b, m)$. It should also be noted that the values $f_1$, $f_2$ and $\Delta f$ must be equal to or bigger than zero. This fact imposes bounds on the magnitude of the location parameter $m$. There are two ways of calculating the estimate $\hat{m}$ of the shift $m$ that are common in literature (Grigoriu 2006). The first lies in $\hat{m} = \min_{1 \le i \le n} y_i$, and the second calculates $\hat{m}$ from $\hat{m} = \hat{\mu} - \hat{a}\hat{b}$. If the second case gives $\hat{m} > \min_{1 \le i \le n} y_i$, we set $\hat{m} = \min_{1 \le i \le n} y_i$. If $\hat{m} < 0$, then we take the resulting estimate equal to $\hat{m} = 0$. According to the analysis of our experimental data, the values $m_{1F}$ and $m_{2F}$ for FDPs proved to be negative, which are explained by data truncation in the lowest limit of our radio instrument, i.e. it is impossible to observe any burst by means of the UTR-2 radio telescope below 9 MHz. Therefore, the PDF parameters of FDPs become $a_{2F} \approx 11.52$, $b_{2F} = 1.76$ MHz, $m_{2F} = 0$ MHz and $a_{1F} \approx 10.69$, $b_{1F} \approx 1.55$ MHz, $m_{1F} = 0$ MHz for starting and ending frequencies, respectively. Fortunately, the instrumental obstacle mentioned above has significantly less impact on the parameter estimates of RDPs. Here we obtain $a_{1R} \approx 7.58$, $b_{1R} \approx 1.58$ MHz and $m_{1R} \approx 12.1$ MHz for lower frequencies whereas for upper frequencies they are $a_{2R} \approx 7.68$, $b_{2R} \approx 1.72$ MHz and $m_{2R} \approx 13.53$ MHz.

Using these results, we can compare the PDFs of FDPs and RDPs. Figure 3 demonstrates how their location depends on frequency. It follows from this that the PDFs are similar and shifted with respect to each other. The occurrence of FDPs is more preferable at lower frequencies of the observations in comparison with RDPs. Besides, there are the observable frequencies where the emergence of RDPs and FDPs are almost equiprobable. Above these frequencies the reverse DPs prevail whereas below the forward DPs dominate. This also indicates the intersection of the histograms shown in Figure 2. To calculate the intersection, we use the following definition (Swain & Ballard 1991)

$$M_{\cap}(f_F, f_R) = \sum_{i}^{n} \min(f_{Fi}, f_{Ri}),$$

where $f_F$ and $f_R$ are two histograms of frequencies with $n$ bins each. Consequently, the intersection peak (at 20–25 MHz on 2015 July 10–12) corresponds to the same amount of FDPs and RDPs (see the bottom panel of Fig. 3). In case of RDPs the bursts were not detected below 12.1 MHz. A similar result was observed in Melnik et al. (2005). Although we have taken $m_{1F} = m_{2F} = 0$ MHz, even without regard to Equation (2), one can assume that FDPs were unlikely to occur below 1.33 MHz, as $\Pr(f < 1.33) \approx 4.7 \times 10^{-9}$. On the other hand, the DP bursts in this observing session probably did not occur above 50 MHz because $\Pr(f > 50) \approx 2.4 \times 10^{-4}$. This sheds light on the ability to detect FDPs below the ionosphere cutoff. It is clear also that the upper and lower frequencies within which DP bursts are observed can vary from one type III burst storm to another.

In this connection, features of start and end frequency distributions of S bursts shown in figure 2 (a) of Morosan et al. (2015) should be pointed out. The histograms are very similar, but their peaks are spaced out. Maybe the random variables satisfy a linear regression, i.e. they have the same PDF with different parameters. It would be interesting to check this remark in the future.

### 3.2 Frequency Drift Rate

The next analysis of DPs is devoted to their frequency drift properties. The data processing procedure was the following. To determine the best function describing the frequency drift of DPs, for each component of the bursts we found the time $t_i$ for each frequency $f_i$ (within the frequency band, where the given DP was detected) corresponding to the "center" of the intensity hump for the DP burst under consideration. Consequently, on the dynamic spectrum of solar radio emission, each such component traces a line itself (see Fig. 4 as an example), and it just characterizes the frequency drift of the chosen DP. Frequency channels of the digital records, clogged by radio narrow-band interferences, were ignored.

Because of radio signal fluctuations, the peak points $(t_i, f_i)$ of DPs often do not lie on a smooth curve. After trial and error, we have chosen a power function for fitting the peak evolution of these bursts in the frequency-time plane. This approach is analogous to the concept used for the study of type II and III bursts proposed in Lobzin et al. (2008, 2010). The fitting function takes the form

$$f(t) = a(t - b)^{-\gamma}, \qquad (6)$$

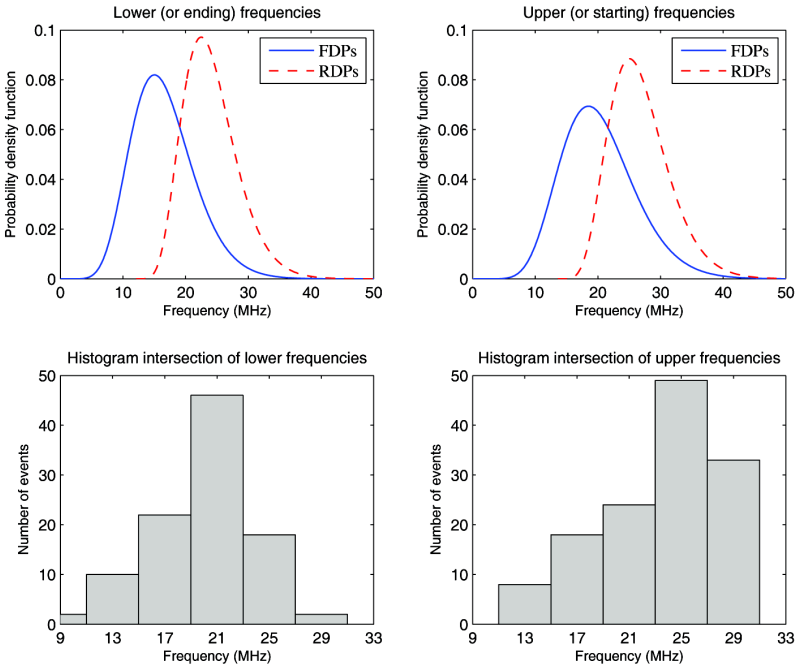


**Fig. 3** PDFs obtained from radio data of FDPs and RDPs for lower and upper frequencies. The bottom pictures show the intersection of the histograms presented in Fig. 2.

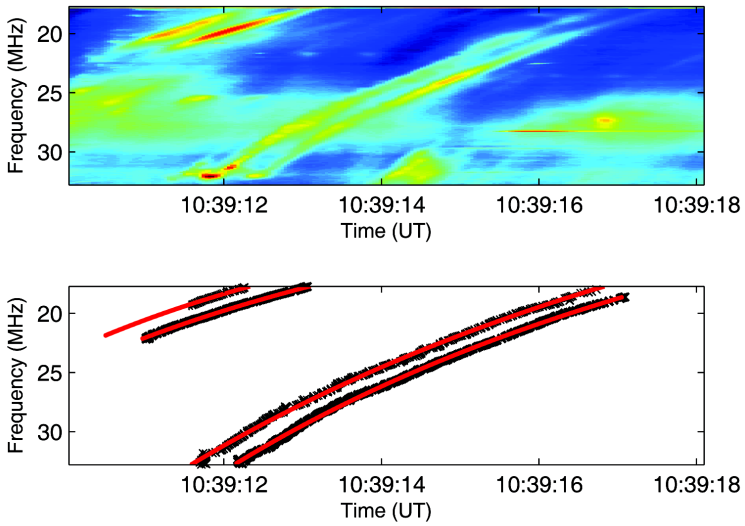


**Fig. 4** Examples of applying the fitting procedure (6) to time-frequency traces of DP peaks.

where $a$, $b$ and $\gamma$ are the parameters leading to the best result (see Fig. 4). It is not difficult to show that in this case the frequency drift rate satisfies the relation

$$\dot{f} = K f^{\nu}\,, \tag{7}$$

where $K$ and $\nu$ are the constants depending only on $a$ and $\gamma$, namely $K = -\gamma a^{-1/\gamma}$ (negative drift rate) and $\nu = 1 + 1/\gamma$. This description is suitable for FDPs, whereas for RDPs in (6) the term $(t-b)$ was replaced by $(b-t)$. Therefore, the sign of $K$ is changed (positive drift rate).

If one finds the peak evolution of FDPs along frequency channels, it is advisable to use the inverse function to (6), i.e.

$$t = b + (a/f)^{1/\gamma}\,. \tag{8}$$

Similarly, the inverse function is derived for fitting the tracks of RDPs with regard to the substitution $(b-t)$. For this issue, the frequency drift rate of each DP is described separately for each of its components by the values of $K$ and $\nu$ themselves. It should be pointed out that long

DPs are most convenient for this analysis. Particularly, the number of such pairs recorded in our observational session was 21 (20 FDPs but only one RDP) with frequency bandwidth ∼8–15 MHz. One of them is shown in Figure 4.

Based on the processing procedure, we have analyzed frequency drift rates of both forward and reverse DPs. Note that the characteristics are not constant for a separate DP in the entire frequency range over which it extends, like the type III bursts, whose drift rate decreases with frequency. Our results are shown in the histograms of Figure 5. In this case each DP is characterized by the frequency drift rate of its components. Their drift rates in each pair are slightly different, although the later component repeats tendencies of the first so that they are still a pair. According to the histograms, the values $K$ and $\nu$ have skewed distributions. They can be characterized by the mean, mode and median (see them in Table 1) which are different for FDPs and RDPs.

### 3.3 Frequency and Time Separations between Pair Components in DPs

One important feature of DPs is the delay time between DP components at the same frequency as well as their frequency separation at the same instant. According to Melnik et al. (2005), for the observational session in 2002, the values of delay time slowly decreased with frequency, varying from 1.4 s to 2.6 s. However, the results have provided an averaged description for many DPs at 12 equidistant frequencies. Using the frequency drift properties of DPs considered above, we can study the frequency and time separations between pair components in each individual burst with higher time and frequency resolutions (recall them, 50 ms and 4 kHz, respectively). For this purpose let us now make use of long DPs. Our results are shown in Figure 6. Generally, they confirm the delay time tendency to decrease with frequency. The frequency separation has the opposite behavior, i.e. the value grows with frequency. Often the tracks demonstrate a monotonic character but sometimes their behavior is like a function with a single local extremum. A more comprehensive analysis of frequency and time separations between pair components for the whole sample of data will be considered elsewhere.

## 4 DISCUSSION

Observations with high spectral and temporal resolutions allow us to measure the characteristics of DPs with rather high accuracy. This can potentially be used to diagnose various parameters of the DP radiation source and to identify the mechanism at the origin of the DP spectral structure. Despite a considerable number of works devoted to this interesting phenomenon, there is no consensus on the DP mechanism. In this section we discuss the main outcomes of our DP burst analysis, which are useful for understanding this phenomenon.

### 4.1 Moving Sources

As has been shown above, the dependence of frequency drift rates of each DP burst on frequency is a power function. Moreover, Equation (7) emphasizes the relationship between DPs and type III solar bursts (see Alvarez & Haddock 1973, Mann et al. 1999). At the same time the observation is not so directly related to the mechanism of generation of type III bursts because not every storm of type III bursts generates DPs. Nevertheless, the source of the DP emission could be connected with plasma emission generated by electron beams moving in solar plasma, and the short life of such bursts might be explained by the disappearance of their sources. If the source has constant velocity $v_0$ and negligible acceleration, then it travels a distance $r(t) = r_0 + v_0(t - t_0)$, where $r_0$ is the initial position and $t_0$ is the starting time (Lobzin et al. 2008). The ambient plasma at the location of the source is characterized by the local plasma frequency in the form $f_p \sim (r/R_\mathrm{s} - 1)^{-\gamma}$, where $R_\mathrm{s}$ is the solar radius. Assuming that the generation of type III solar bursts occurs at plasma frequency or its harmonics, it is not difficult to obtain expressions like (6)-(7). On the other hand, the frequency drift rate is written as

$$\dot{f} = f\,\frac{1}{2N_\mathrm{e}}\,\frac{dN_\mathrm{e}}{dr}\,v_\mathrm{s}\,, \tag{9}$$

where $v_\mathrm{s}$ is the source velocity projected along the radial direction, and $N_\mathrm{e}$ describes the electron density at the location of the source. In this framework our experimental data indicate that the source velocities were more diverse in values than conventional type III electron velocities. Recall that Alvarez & Haddock (1973) obtained the relation $df/dt = -0.01 f^{1.84}$ for many solar type III bursts in the frequency range from 75 kHz to 550 MHz. In a more recent study of Mann et al. (1999) these bursts come after $df/dt = -0.0074 f^{1.76}$. The absolute frequency drift rates of DPs may be both lower and significantly higher than those in ordinary solar type III bursts. Therefore, a promising explanation of this effect should be sought in the theory of Zaitsev & Levin (1978). At present it allows one to explain most experimental results obtained for DPs. The approach is based on the excitation of plasma waves in those layers of the corona where the condition of double plasma resonance is satisfied.

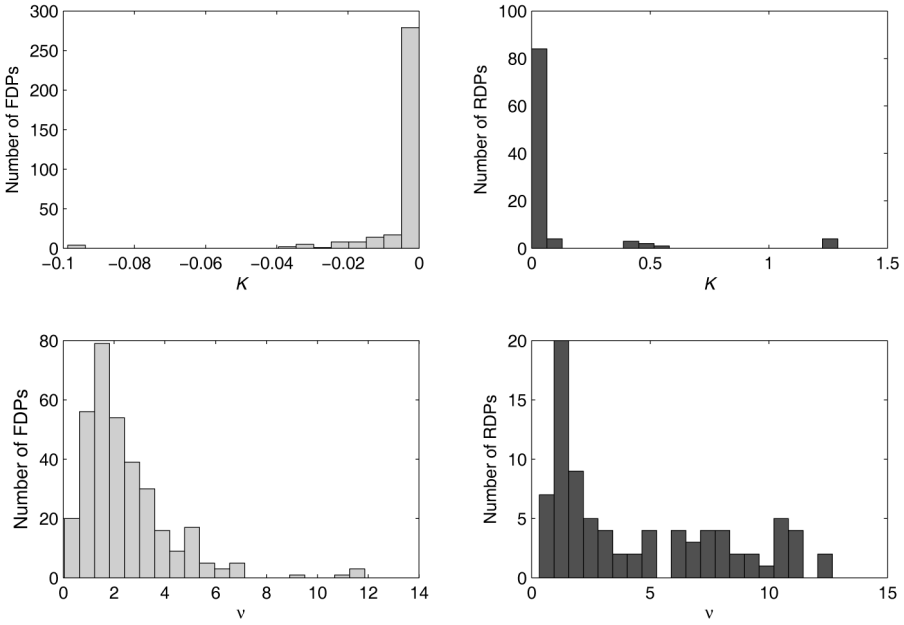


**Fig. 5** Histograms of the parameters $K$ and $\nu$ for FDPs and RDPs, respectively. Their values enter into Equation (7).

**Table 1** Probabilistic Properties of FDPs and RDPs shown in the above Histograms (Fig. 5)

| | Parameters of Equation (7) for DPs observed on 2015 July 10–12 | | | | | |
|---|---|---|---|---|---|---|
| | $K$ | | | $\nu$ | | |
| | Mean | Mode | Median | Mean | Median | Mode |
| FDPs | –0.0045 | –0.002 | –0.0011 | 2.45 | 1.93 | 1.32 |
| RDPs | 0.0502 | 0.045 | $\approx 0$ | 4.57 | 2.88 | 1.21 |

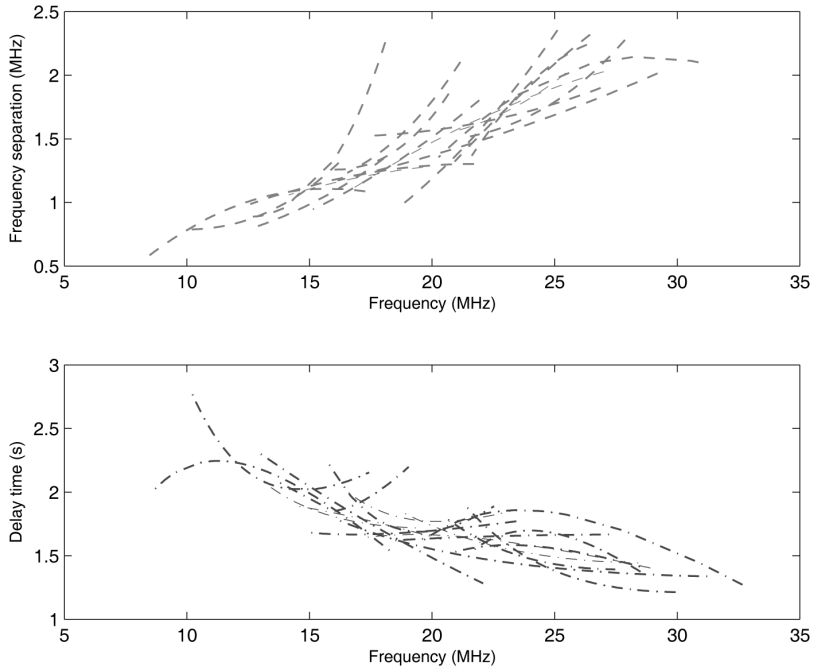


**Fig. 6** Top panel shows the frequency interval between components of long FDPs, and bottom panel is the delay time vs. frequency dependence for those very bursts.

### 4.2 Double Plasma Resonance

Now the model of double plasma resonance, allegedly responsible for the formation of zebra structure, is the most popular and well-developed (see, for example, the recent review of Zheleznyakov et al. 2016). It is assumed that accelerated electrons with an anisotropic distribution generate longitudinal plasma (upper hybrid) waves with frequency near the so-called upper hybrid frequency $f_{UH} = \sqrt{f_p^2 + f_B^2}$. As has been shown by Kuijpers (1975), as well as by Zhelezniakov & Zlotnik (1975), the generation efficiency of upper-hybrid waves increases significantly, if their frequency is close to the harmonics of the electron cyclotron frequency $f_B$, i.e. the condition

$$f_{UH} = \sqrt{f_p^2 + f_B^2} \simeq s f_B$$

is valid for $s = 2, 3, 4, \ldots$ Upper-hybrid waves are then transformed into radio emission due to nonlinear processes (such as scattering of plasma waves by ions). Following the arguments of Zaitsev & Levin (1978), the sign of the frequency drift rate of DPs depends on the local value of the gradients $1/2N_{\rm e}\,(\partial N_{\rm e}/\partial z)$ and $1/H\,(\partial H/\partial z)$, where $H$ is the magnetic field strength and $z$ the distance from the injection region. Thus the mechanism can generate DP bursts with both forward and reverse frequency drift, including the case of vertical DPs. As has been shown above, the frequency interval between two components in each DP at the same time increases with increasing frequency. Probably, this tendency indicates a decay of the magnetic field strength with height in the solar corona.

Although the exact height distributions of the magnetic field and the plasma density in the solar corona are unknown, the use of certain reasonable assumptions (for example, magnetic fields obtained by extrapolating photospheric magnetograms) makes it possible to reproduce the observed spectra of zebra structures and the position of the sources of their bands. The advantage of the double plasma resonance model is its versatility and flexibility. By selecting suitable magnetic field profiles and plasma densities, virtually any spectrum (with any frequency distribution of the emission bands) can be obtained. Thus, the diagnosis of source parameters by radio observations requires the involvement of additional data or some assumptions about the structure of the source. To form a pronounced DP structure, the radiation must be generated in a relatively narrow magnetic tube. Otherwise, transverse inhomogeneities in the plasma and magnetic field would lead to broadening and fusion of the DP components. Sometimes the effects are observable. The difference in behavior of FDPs and RDPs in histograms of starting and ending frequencies shows that FDPs and RDPs were generated in different (but probably overlapping) regions of the solar corona. Recall also that if the number of RDPs recorded by Suzuki & Gary (1979) exceeded the number of FDPs in order of magnitude, then our data indicate the opposite situation, i.e., FDPs were detected more often. The difference is explained by the frequency range of observations (24.7–74 MHz and 9–33 MHz, respectively).

## 5 CONCLUSIONS

Following this study, we have established that neither Equation (1) nor Equation (2) are precisely suitable for the description of frequency drift rates of DP components observed on 2015 July 10–12. Our comprehensive analysis clearly shows that the dependence of functional form of frequency drift rate for DPs on frequency is similar to the case of type III solar bursts (Alvarez & Haddock 1973, Mann et al. 1999), but the model parameters are different. Finally it should be noticed also that although our fitting model (7) is close to the representation (2) from Melnik et al. (2005), the advantage of our approximation is that it uses a minimal number of parameters. Probably, the increase in the number of required parameters in (2) is because the DP data set of 2002 was obtained basically by an analog multichannel receiver with frequency bandwidth 3 kHz in each frequency channel. Consequently, the data contained notable omissions. In addition, the frequency drift rate of DPs was estimated by averaging over all observable bursts having different rates.

In this work we have shown that upper and lower frequencies at which DPs occur as well as their total frequency bandwidth are random variables satisfying a shifted gamma distribution. Deviations from this distribution are due to the limited frequency band. Therefore, a part of the DP sample was not received by our instrument, and our records were truncated and incomplete. Nevertheless, this did not prevent us from performing a statistical analysis on DP properties. We have found that the PDFs of FDPs and RDPs are similar, but their peaks are shifted in frequency. In our observations the largest number of RDPs has been detected at the top of the UTR-2 frequency range, whereas the largest number of FDPs has been noticed near the lowest frequencies available. It should be pointed out that this was achieved due to the uniform amplitude-frequency response of our instrument. In the future we are going to provide updated observations by means of the new ultra-wideband radio telescope called the Giant Ukrainian Radio Telescope (GURT), which is being built now in

Ukraine (Konovalenko et al. 2016). It has a wider frequency band (than its predecessor, UTR-2) for solar observations (from 10 to 80 MHz) that will be enough to cover a wider frequency range of solar radio emission where DPs occur. We hope that such observations will be extended which will add to our knowledge about frequency-time properties of DPs.

**Acknowledgements** We want to thank the GOES, STEREO and SOHO teams for developing and operating the instruments as well as for their open data policy. This research was also partially supported by Research Grant 0117U002396 from the National Academy of Sciences of Ukraine. The authors are grateful to Dorovskyy V.V. for useful discussions.

## References

Alvarez, H., & Haddock, F. T. 1973, Sol. Phys., 29, 197

Braude, S. I., Megn, A. V., Riabov, B. P., Sharykin, N. K., & Zhuk, I. N. 1978, Ap&SS, 54, 3

de La Noe, J., & Moller Pedersen, B. 1971, A&A, 12, 371

Feller, W. 2008, An Introduction to Probability Theory and Its Applications, 2 (John Wiley & Sons)

Grigoriu, M. 2006, Probabilistic Models for Directionless Wind Speeds in Hurricanes (US Department of Commerce: NIST GCR 06-906)

Jester, S., & Falcke, H. 2009, New Astron. Rev., 53, 1

Johnson, N. L., Kotz, S., & Balakrishnan, N. 1970, Distributions in Statistics: Continuous Univariate Distributions, 2 (Boston: Houghton Mifflin Company, MA.)

Konovalenko, A., Sodin, L., Zakharenko, V., et al. 2016, Experimental Astronomy, 42, 11

Krymkin, V. V. 1971, Radiophysics and Quantum Electronics, 14, 161

Kuijpers, J. 1975, A&A, 40, 405

Lobzin, V. V., Cairns, I. H., & Robinson, P. A. 2008, ApJ, 677, L129

Lobzin, V. V., Cairns, I. H., Robinson, P. A., et al. 2010, ApJ, 724, 1099

Mann, G., Jansen, F., MacDowall, R. J., Kaiser, M. L., & Stone, R. G. 1999, A&A, 348, 614

McConnell, D. 1982, Sol. Phys., 78, 253

Melnik, V. N., Konovalenko, A. A., Dorovskyy, V. V., et al. 2005, Sol. Phys., 231, 143

Moller-Pedersen, B., Smith, R. A., & Mangeney, A. 1978, A&A, 70, 801

Morosan, D. E., Gallagher, P. T., Zucca, P., et al. 2015, A&A, 580, A65

Roberts, J. A. 1958, Australian Journal of Physics, 11, 215

Ryabov, V. B., Vavriv, D. M., Zarka, P., et al. 2010, A&A, 510, A16

Singh, V. P. 1998, in Entropy-Based Parameter Estimation in Hydrology (Boston: Kluwer Academic Publishers)

Stanislavsky, A. A., Konovalenko, A. A., Rucker, H. O., et al. 2009, Astronomische Nachrichten, 330, 691

Suzuki, S., & Gary, D. E. 1979, Proceedings of the Astronomical Society of Australia, 3, 379

Swain, M. J., & Ballard, D. H. 1991, International Journal of Computer Vision, 7, 11

Zaitsev, V. V., & Levin, B. N. 1978, Soviet Ast., 22, 223

Zhelezniakov, V. V., & Zlotnik, E. I. 1975, Sol. Phys., 43, 431

Zheleznyakov, V. V., Zlotnik, E. Y., Zaitsev, V. V., & Shaposhnikov, V. E. 2016, Physics Uspekhi, 59, 997